CHEMPHYSCHEM

DOI: 10.1002/cphc.200900119

SERS Microscopy: Nanoparticle Probes and Biomedical Applications

Sebastian Schlücker*[a]

SERS Microscopy:
Nanoparticle Probes and
Biomedical Applications

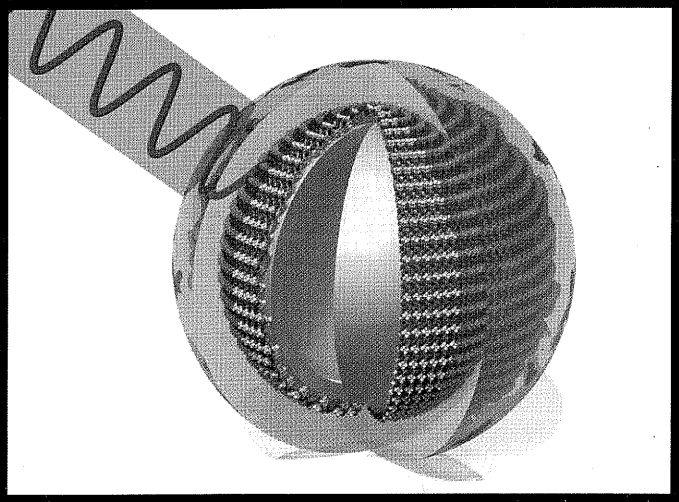

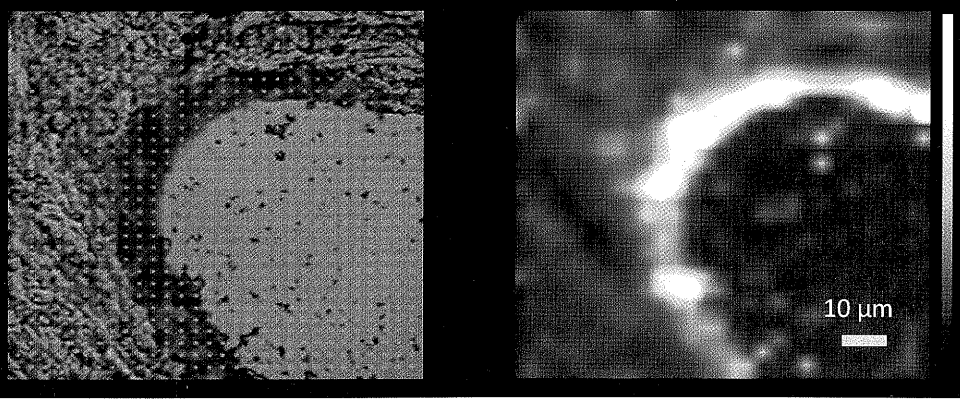

Surface-enhanced Raman scattering (SERS) microscopy is a novel method of vibrational microspectroscopic imaging for the selective detection of biomolecules in targeted research. This technique combines the advantages of biofunctionalized metal nanoparticles and Raman microspectroscopy for visualizing and quantifying the distribution of target molecules such as proteins in cells and tissues. Advantages of SERS over existing labeling approaches include the tremendous multiplexing capacity, quantification using the characteristic SERS signatures and high photostability. This review summarizes current designs of nanoparticle-based SERS probes and highlights first biomedical applications of SERS microscopy for protein localization ex and in vivo.

1. Introduction

Surface-enhanced Raman scattering (SERS) is an ultra-sensitive vibrational spectroscopic technique for the detection of molecules on or nearby the surface of plasmonic nanostructures.[1–3] Numerous applications have demonstrated the potential of SERS for the label-free detection of various analytes. More recently, SERS is increasingly used as a readout method for the selective and sensitive detection of proteins and oligonucleotides.[4] This approach requires SERS-labeled (bio)molecules with a high binding affinity to the corresponding target, that is, SERS-active probes or SERS labels have the same function as external chromophores such as dyes and fluorophores. Target localization in SERS microscopy is achieved by spatially resolved detection schemes, using the characteristic vibrational Raman spectrum of the corresponding SERS label for identification. SERS microscopy as a novel methodology of Raman microscopy for targeted research therefore combines concepts known from fluorescence microscopy and conventional vibrational imaging: labeled biomolecules for molecular recognition together with vibrational microspectroscopy for detection and localization (Figure 1).

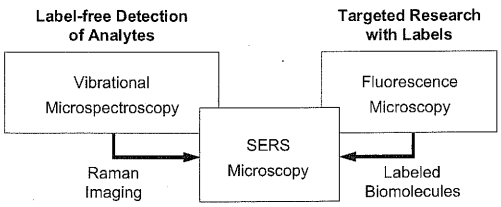

Figure 1. SERS microscopy is a novel method of vibrational microspectroscopy for the selective detection of biomolecules in targeted research. This technique combines the advantages of Raman imaging and biofunctionalized metallic nanoparticles for visualizing and quantifying the distribution of target molecules such as proteins in cells and tissue specimens.

In this review, current designs of SERS probes based on metallic nanoparticles will be summarized. The primary aim is to introduce relevant physical and chemical concepts, in particular those which are important for parameters such as sensitivity, multiplexing (parallel detection) and quantification. Topics such as plasmons in metallic nanospheres and their role in enhancing the Raman scattering of molecules on their surface (Section 2) as well as the importance of surface coverage and encapsulation (Section 3) are discussed. Then, first biomedical applications of SERS microscopy for protein localization ex and in vivo are highlighted (Section 4). Applications of SERS for the selective detection of proteins and nucleic acids in solution have been summarized recently[4] and will therefore not be discussed here; the specific requirements for examining biological samples, however, apply for both SERS-based assays[5] and SERS microscopy.[6]

2. Surface-Enhanced Raman Scattering

SERS is observed for molecules on or nearby the surface of metallic nanostructures that can support localized surface plasmon resonances (SERS substrate). The signal levels observed in SERS are several orders of magnitude higher than in conventional Raman scattering, providing the sensitivity required for bioanalytical and biomedical applications.[1–3]

The dominant contribution leading to this drastic signal increase arises from the electromagnetic enhancement mechanism (Section 2.1). The high sensitivity of SERS can be exploited either for the label-free detection of analytes or in targeted research with SERS labels (Section 2.2).[7]

2.1. Electromagnetic Enhancement Mechanism

Plasmons (plasma oscillations) of the conduction electrons in metallic nanostructures can be resonantly excited in the visible region of the electromagnetic spectrum.[1–3] The excitation of the plasmon resonance is a necessary condition for the observation of SERS. The dominant contribution to the drastic signal enhancement in SERS is due to an electromagnetic mechanism, which is schematically shown in Figure 2. The nanosphere in the center has a diameter ($d=2r_a$) smaller than the wavelength of the incoming electromagnetic field E_0. The parameter R indicates the distance between the center of the nanosphere and the molecule. Elastic scattering of the incident field E_0 off the metal sphere leads to a field enhancement by the additional component E_{LM}. The resulting incoming field $E_{in}=E_0+E_{LM}$ induces a dipole moment μ_{ind} in the molecule. E_{in} and μ_{ind} are vectorial properties which are connected by the molecular polarizability tensor α. The induced molecular dipole moment μ_{ind} oscillates with different frequency components: ω_0 (Rayleigh, elastic scattering), $\omega_0+\omega_R$ (anti-Stokes, inelastic scattering) and $\omega_0-\omega_R$ (Stokes, inelastic scattering), where ω_0

[a] *Prof. S. Schlücker*
Department of Physics, University of Osnabrück
D-49069 Osnabrück (Germany)
Fax: (+49) 541-969-13592
E-mail: sebastian.schluecker@uos.de

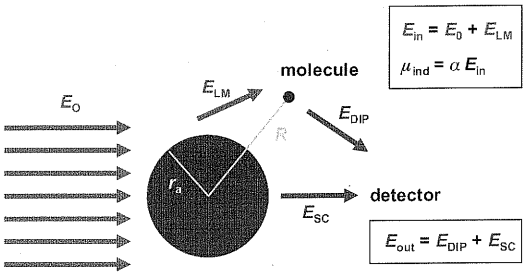

Figure 2. Electromagnetic enhancement mechanism in SERS. The electric field E_0 of the laser is elastically scattered off the metal nanosphere with radius r_a. The total incoming field $E_{in}=E_0+E_{LM}$ induces a dipole moment $\mu_{ind}=\alpha E_{in}$. The polarizability α is a tensor of rank 2. The emitted dipolar radiation E_{DIP}, which is red-shifted in the case of Stokes scattering, is also elastically scattered off the metal nanosphere. Both field components, E_{DIP} and E_{SC} add up to the outgoing field E_{out}.

and ω_R are the angular frequencies of the incoming laser field and of the corresponding normal mode, respectively. In the case of Stokes scattering with angular frequency $\omega_0-\omega_R$, the emitted dipole radiation E_{DIP} is red-shifted with respect to the incident laser wavelength ω_0. Elastic scattering of E_{DIP} off the metal sphere causes an enhancement by the additional component E_{SC}, resulting in an outgoing field $E_{out}=E_{DIP}+E_{SC}$. In summary, for both the incoming and outgoing electric field, E_{in} and E_{out}, the enhancement originates from elastic scattering off the metal sphere. In this simple electromagnetic model, the SERS intensity is proportional to $I_{in}\cdot I_{out}$, where I denotes the detected intensity $I=|E|^2$, and the enhancement decreases with $(r_a/R)^{-12}$.[3] This strong distance dependence leads to the observed surface selectivity in SERS: only molecules on or very close to the nanoparticle surface experience the enormous field enhancement. Additionally, the orientation of the adsorbed species has to be considered. Adsorption of molecules to the surface of plasmonic nanostructures is therefore a key step in most analytic applications of SERS. Details on the theory of SERS are summarized in two recent monographs.[1–2]

Sebastian Schlücker (born 1973) studied chemistry in Würzburg (Germany) and Swansea (UK), and received his Dr. rer. nat. (PhD) in Biophysical Chemistry with Wolfgang Kiefer from Würzburg University in 2001. He did his postdoctoral research in biomedical vibrational microspectroscopic imaging with Ira Levin at the National Institutes of Health (Bethesda, MD, USA), and then started a research group at Würzburg University. After his habilitation and a short period as a Heisenberg fellow of the Deutsche Forschungsgemeinschaft, he joined the Physics Department at Osnabrück University as an Associate Professor (W2) in 2008. The Schlücker research group develops agents and optical methods for biomedical diagnostics, and investigates hydrogen bonding and molecular recognition with laser spectroscopic techniques.

2.2. Label-Free Detection versus Targeted Research with SERS

There are two fundamentally different applications of SERS with metallic nanoparticles as SERS substrates: the label-free detection of analytes (Figure 3, left) and targeted research with

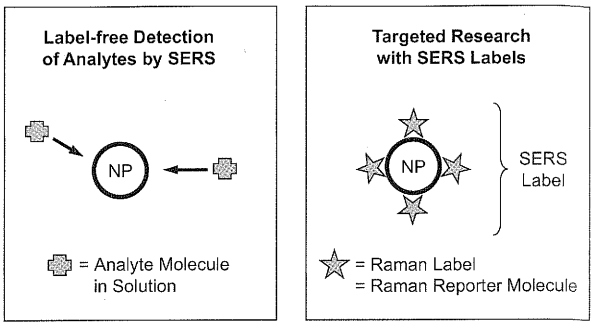

Figure 3. Two different modalities of using metal nanoparticles (NPs) as SERS substrates.[7] Left: The label-free detection of analytes from solution phase is based on their characteristic SERS spectrum after adsorption onto the particle surface. Right: Targeted research uses SERS labels for the identification of (bio)molecules, based on the characteristic signature of Raman reporter molecules adsorbed onto the particle surface.

SERS labels (Figure 3, right).[7] Currently, the label-free detection of an analyte is the most widely used approach: the identification is based on the characteristic SERS spectrum of the analyte when it is adsorbed onto the surface of the colloidal particle. The second approach is to use the metallic nanoparticles in combination with Raman labels as SERS labels (Figure 3, right): the organic Raman reporter molecules are (ideally permanently) adsorbed on the surface, giving rise to the characteristic SERS signature which is necessary for the indirect identification of the target molecule.

Enzymes, dyes, molecular fluorophores and quantum dots are well known labeling agents for the selective detection of biomolecules.[8] SERS nanoparticle probes, although relatively large with a diameter of typically 20–100 nm, represent a novel and attractive method for labeling proteins and nucleic acids.[9–18] Advantages of SERS over existing labeling approaches include: the tremendous multiplexing capacity for simultaneous target detection due to the small linewidth of vibrational Raman bands; quantification using the characteristic SERS spectrum of the corresponding label; the need for only a single laser excitation wavelength; high photostability and optimal contrast by using red to near-infrared excitation in order to minimize the disturbing autofluorescence of cells and tissues. Examples in Sections 3 and 4 illustrate some of these advantages.

3. Functionalized Metal Nanoparticles as SERS Probes

Functionalized metal nanoparticles for targeted research contain three constituents (Table 1): a SERS substrate (Section 3.1),

Table 1. SERS substrate, Raman label and biomolecule are the building blocks of target-specific metal nanoparticles. Their respective function together with examples are also listed. The combination of SERS substrate and Raman label or Raman reporter molecule is called SERS label.

	Component	Function	Examples
SERS label	SERS substrate	Sensitivity: Raman signal enhancement	Ag, Au, Au/Ag nanoparticles
	Raman label	Identification: characteristic Raman signature	Mercaptobenzoic acid (SERS), rhodamine 6 G (SERRS)
	Biomolecule	Selectivity: specific target recognition	Antibodies, aptamers

Raman labels adsorbed onto its surface (Section 3.2) and biomolecules for target-specific binding attached to the SERS label (Section 3.3).

3.1. Metallic Nanoparticles as SERS Substrates

The first step in the design of SERS labels (Table 1) is to choose and prepare a suitable SERS substrate because the metallic nanoparticles should possess certain optical properties in order to provide the necessary signal enhancement required for sensitivity. The synthesis of metal colloids (Section 3.1.1) and their optical properties (Section 3.1.2) are discussed.

3.1.1. *Synthesis of Metallic Nanoparticles*

For an introduction to the topic of colloidal SERS substrates, a recent monograph by Aroca is recommended.[1] Numerous protocols for the synthesis of metallic nanoparticles are available.[19,20] Many of them use metal salts which are reduced in the presence of a stabilizer. Silver and gold nanospheres are the most commonly used SERS substrates. As an example, the preparation of gold/silver nanoshells according to a procedure described by Xia and co-workers is discussed because they exhibit tunable plasmon resonances in the red to near-infrared (NIR) with high scattering efficiencies.[21,22] Silver nanospheres are produced in a polyol process, using silver nitrate dissolved in ethylene glycol together with polyvinylpyrrolidone (PVP). The silver particles then serve as a template for the formation of hollow gold/silver spheres upon addition of Au^{3+} ions. In this template-based replacement reaction, three silver atoms of the particle are replaced by one gold atom according to the following stoichiometry: $3\,Ag(s) + Au^{3+}(aq) \rightarrow 3\,Ag^{+}(aq) + Au(s)$. The shell thickness of the gold/silver alloy depends on the relative amount of gold being added: the shell thickness decreases with an increasing amount of gold, resulting in a red shift of the plasmon band.[22]

In general, parameters such as size, shape and chemical composition determine the optical properties of metal nanoparticles and are therefore important for a rational design of efficient SERS probes. For quantitative SERS, monodisperse particles are desired: a narrow size distribution guarantees similar scattering intensities (cf. Figure 2) and thus comparable SERS intensities. Methods for the controlled synthesis of monodisperse nanoparticles, in particular for Ag and Au, are therefore highly desirable in order to achieve quantitative SERS.

3.1.2. *Plasmon Resonances in Metallic Nanospheres*

The extinction maximum of silver and gold nanospheres occurs in the blue to green part of the electromagnetic spectrum, while the plasmon resonance of gold/silver nanoshells can be tuned over the red to near-infrared region (Figure 4).

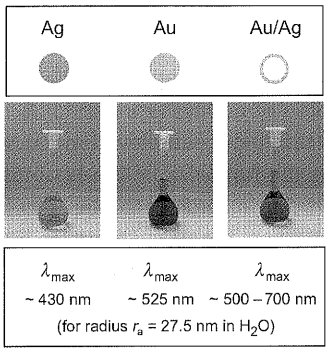

Figure 4. Different metal nanoparticles together with the calculated positions of their plasmon resonances λ_{max} for a radius of $r_a = 27.5$ nm in water. Left: Silver nanospheres with $\lambda_{max} \sim 430$ nm. Middle: Gold nanospheres with $\lambda_{max} \sim 525$ nm. Right: Gold/silver nanoshells of this size have tunable plasmon resonances in the range $\lambda_{max} \sim 500$–700 nm.

The position of the plasmon peak, λ_{max}, depends on a number of parameters, in particular the size of the nanospheres and the dielectric function of both the metal sphere and the surrounding medium. Figure 4 bottom shows calculated λ_{max} values for 55 nm metal spheres in water.

Optical excitation of plasmons is achieved either by tuning the laser wavelength to the plasmon resonance for a given colloid, or vice versa, by shifting the plasmon band into resonance with a certain laser wavelength. Experimentally detected extinction spectra of metal colloids in the UV/Vis region contain both absorption and scattering contributions; the latter determines the SERS efficiency of single colloidal particles.

The optical properties of spheres can be calculated using Mie theory, also called Lorenz-Mie theory.[23,24] Figure 5 shows the results from Mie calculations for a single 55 nm gold sphere and a single 55 nm gold/silver nanoshell with shell thickness $d = 5$ nm, both with water as surrounding medium. Each extinction spectrum is the sum of the absorption and scattering contributions. As discussed above and shown in Figure 5, gold/silver nanoshells exhibit plasmon resonances at higher wavelengths; according to these Mie calculations, their scattering intensity is higher compared with gold spheres. In both cases absorption is larger than scattering. For single silver

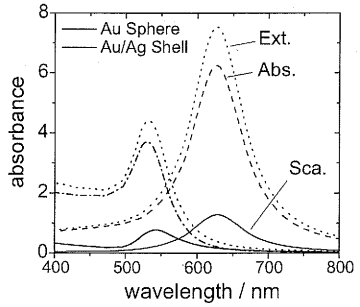

Figure 5. Extinction spectrum (=absorption + scattering contributions) of a single Au nanosphere (r_a=27.5 nm) in comparison with a single Au/Ag nanoshell (r_a=27.5 nm, d=5 nm) calculated by Lorenz-Mie theory with water as the surrounding medium (Ext.=Extinction; Abs.=Absorption; Sca.=Scattering). The Au/Ag nanoshell exhibits a plasmon peak at a higher wavelength λ_{max} and has a larger scattering efficiency compared with the Au nanosphere of the same size.

nanoparticles (data not shown, cf. Figure 4), plasmon resonances are typically observed between 390–450 nm, with very large scattering contributions favorable for SERS.[1,2] Therefore, silver is the most commonly employed metal in SERS.

Figure 6 shows the tunability of the plasmon band in single metallic nanoparticles according to Mie calculations. For gold and silver nanospheres, the wavelength of the plasmon band

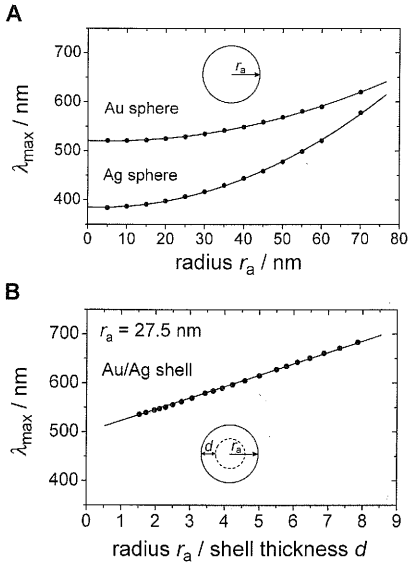

Figure 6. A) Position of the plasmon bands for Au and Ag nanospheres in water as a function of radius r_a. B) Position of the plasmon band for Au/Ag nanoshells in water as a function of shell thickness d for a constant radius of r_a=27.5 nm.

is plotted as a function of the particle radius r_a (Figure 6A). The plasmon resonance for gold occurs at higher wavelengths compared with silver spheres (cf. also Figure 4). For gold/silver nanoshells, the plasmon band is shifted to even higher wavelengths and can be tuned over the entire red to NIR range (Figure 6B). By using red laser excitation (632.8 nm), it has been shown experimentally that 60 nm gold/silver nanoshells yield ca. 8 times higher SERS intensities compared with gold nanospheres of the same size.[18] In addition to the nanoshells with a solvent core and a gold/silver alloy shell discussed here, also other core/shell structures, such as SiO_2/Au, Ag/Au and Au/Ag core/shell particles, are used as SERS substrates.[25–27] Mirkin and co-workers, for example, have introduced silver staining of small functionalized gold nanoparticle probes to produce the actual SERS substrate.[11]

Generally, the interest in using plasmonic nanostructures as efficient SERS substrates in combination with red to near-infrared laser excitation is often triggered by its use in biomedical and biological applications. The minimization of disturbing autofluorescence of biological specimens leads to an improved image contrast which may be more important than the maximization of absolute SERS signal levels. For optical applications in vivo it is additionally essential to pass tissue such as the skin barrier, taking advantage of the "biological window" in the near-infrared.

3.2. SERS Labels: SERS Substrates Covered with Raman Labels

The second step in the design and preparation of SERS labels (Table 1) is to chemically conjugate SERS-active metal particles with the desired optical properties to Raman reporter molecules with a characteristic spectral signature.

Generally, efficient SERS requires the presence of molecules on or nearby the surface of a SERS substrate (cf. Figure 2). The signal level increases with the number of molecules adsorbed onto the particle surface. Nitrogen- or sulfur-containing molecules are very often employed because of their affinity to silver and gold, respectively. SERS labels, the combination of SERS substrate and Raman label (Table 1), consist either of single (Section 3.2.1) or multiple (Section 3.2.2) metal nanoparticles.

3.2.1. Single Nanoparticle-Based SERS Probes: Surface Coverage and Encapsulation

Three different SERS label designs based on single metallic nanoparticles as SERS substrates are shown in Figure 7. Porter and co-workers have introduced aryldisulfides as Raman labels because they form a monolayer attached to the surface via

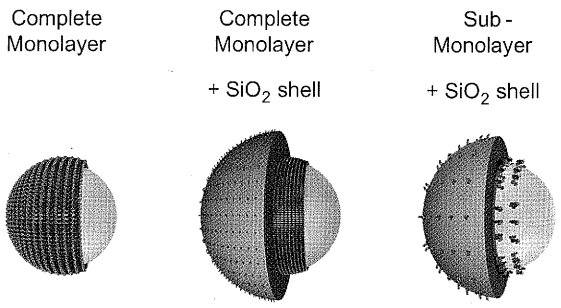

Figure 7. Single SERS particle probes differing in surface coverage and encapsulation. Left: Complete monolayer without protective encapsulation.[9,12] Middle: Complete monolayer coverage with protective silica shell.[18] Right: Sub-monolayer coverage with protective silica shell.[7,29]

stable Au–S bonds (Figure 7, left).[5,9,12] A self-assembled monolayer (SAM) provides several advantages with respect to sensitivity, quantification and multiplexing. The high sensitivity arises from the maximum surface coverage with Raman reporter molecules in a complete SAM (Figure 7, left and middle) compared with sub-monolayer coverage (Figure 7, right).[18] Additionally, molecules within a SAM are usually uniformly oriented with respect to the surface normal. This leads to reproducible SERS signatures with only few dominant Raman bands,[18] which is beneficial for quantification and multiplexing. A SAM possesses also a protective function because it minimizes co-adsorption of other molecules onto the surface of the SERS substrate, thereby reducing disturbing spectral interferences caused by other molecules.

Encapsulation can completely eliminate this issue by avoiding desorption (of Raman labels from the metal surface) and adsorption (of molecules from the environment to the surface). Different encapsulation materials are available, including proteins as biopolymers,[14] organic polymers[17,28] and silica.[7,18,29,31] In particular silica is attractive because of its high mechanical stability and the option for long-term storage.

Mulvaney, Natan and co-workers have introduced the concept of silica encapsulation for SERS nanoparticle probes (Figure 7, right).[29] Co-adsorption of Raman labels and SiO_2 precursors (typically in a 1:20 stoichiometry) leads to a sub-monolayer coverage of the surface with Raman reporter molecules, followed by silica encapsulation.[30] Soon after, Doering and Nie presented a very similar approach to glass-coated nanoparticles.[31] Generally, a glass shell provides unique advantages: it protects the SERS label both chemically and physically. For example, a 20 nm shell of silica leads to a significantly increased lifetime of gold nanospheres in the presence of *aqua regia*: 3 h in comparison to 15 sec for the bare Au colloid.[29] Storage stability and protection against mechanical deformation are further advantages.

Schlücker and co-workers have introduced the concept of silica-encapsulated SERS probes comprising a SAM (Figure 7, middle), thereby combining the chemical and spectroscopic advantages of both—a protective silica shell and a complete self-assembled monolayer of Raman labels.[18] In contrast to the sub-monolayer coverage with Raman labels, a SAM leads to a higher sensitivity. Using gold/silver nanoshells and red laser excitation (632.8 nm), it has been shown experimentally that a complete SAM yields ca. 22 times more intense signals compared with sub-monolayer coverage.[18] For a subsequent silica encapsulation of the SAM, SiO_2 precursors may not directly adsorb onto the particle surface because the metal surface is already completely covered with organic molecules, that is, the Raman labels. This problem can be overcome in various ways, for example, by using polyelectrolyte layers with alternating charges (layer-by-layer deposition) in combination with a modified Stöber method.[30] Functionalization of the glass surface, for example with amino groups, allows the subsequent conjugation of biomolecules to silica-encapsulated SERS labels.[18]

3.2.2. Aggregates and Assemblies of Metal Nanoparticles as SERS Probes

Very high SERS intensities can be observed for nanoparticle aggregates (Figure 8, left). This is attributed to the presence of molecules in or near junctions between particles, where the

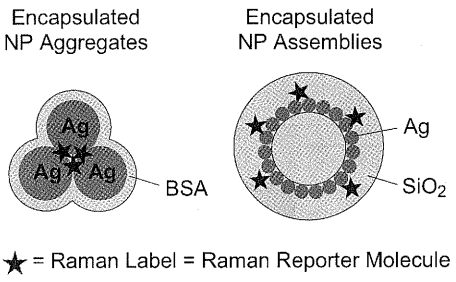

Figure 8. Left: Protein (BSA)-encapsulated aggregates of metal nanoparticles.[14] Right: Silica (SiO_2)-encapsulated assemblies of metal nanoparticles.[15]

electromagnetic field enhancement may be increased by several orders of magnitude. Particle aggregation is initiated very easily (but is not necessarily desired), for example, simply by changing the solvent. In contrast, control over particle aggregation is more difficult to achieve. The Biomedical/Life Sciences Division of the Digital Health Group, Intel Corporation, for example, has introduced a concept for the Raman label-induced, controlled aggregation of silver particles called COINs (composite organic–inorganic nanoparticles).[14] A shell of bovine serum albumin (BSA) protects the COINs and allows further conjugation chemistry.

Nanoparticle assemblies (Figure 8, right) are an alternative to aggregates. Kim and co-workers demonstrated the preparation of silica-encapsulated assemblies.[15] Here, 180–210 nm silica particles serve as a template for the deposition of many small Ag particles onto its surface, followed by the adsorption of Raman labels and subsequent encapsulation with silica. This leads to relatively well defined assemblies, in particular because of the monodisperse and perfectly spherical silica templates resulting from the Stöber method. The overall size of the assemblies is approx. 250 nm and they also have been used for targeted cellular research.

3.3. Biofunctionalized SERS Probes

Bioconjugation is the third step in the design and preparation of target-specific SERS probes, independent of the type or size of a particular SERS label. Specifically, SERS labels must be conjugated to target-specific probe molecules (Table 1) such as antibodies for antigen recognition.

3.3.1. Conjugation of Biomolecules to SERS Labels

In summary, the selective detection of biomolecules such as proteins and nucleic acids by SERS nanoparticle probes requires the following components (see Table 1): i) a metallic nanoparticle for signal enhancement, for example Ag, Au or

Au/Ag nanospheres; ii) a Raman label with a characteristic vibrational signature such as mercaptobenzoic acid for SERS or dyes such as Rhodamine 6G for SERRS (surface-enhanced resonance Raman scattering);[32] iii) a biomolecule such as an antibody for specific binding to the corresponding target molecule.

The synthesis of biofunctionalized SERS probes starts with the preparation of metal colloids (Section 3.1.1 and Figure 9, left). The addition of Raman labels to the nanoparticles leads

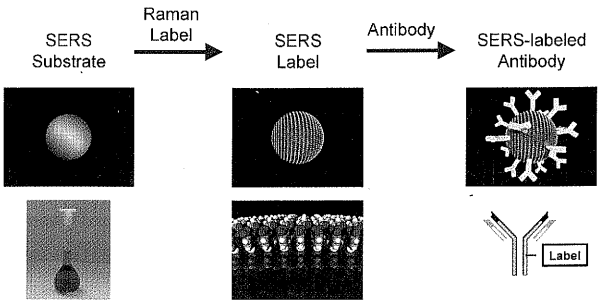

Figure 9. Synthesis of SERS-labeled antibodies. SERS substrates are incubated with Raman labels. The resulting SERS label is then conjugated to antibodies.

to the formation of SERS labels (Figure 9, middle); in the case of gold particles and arylthiols, a self-assembled monolayer (SAM) is formed. Encapsulation of the SERS label, primarily for protection, is an optional additional step which is often desirable. Materials such as silica, proteins and synthetic polymers can be employed as encapsulants. Numerous protocols for subsequent bioconjugation are available:[33] biomolecules can be (covalently) attached either to the encapsulant or, in the absence of a protective shell, directly to the Raman labels. A textbook example of bioconjugation chemistry is the activation of carboxylic acids (e.g. on the surface of SERS labels) by *N*-hydroxysuccinimide (NHS). The resulting NHS esters are then, for example, conjugated to primary amines such as lysine residues in proteins.[33] Conjugation of the SERS label to the antibody yields the SERS-labeled antibody (Figure 9, right).

3.3.2. Raman Spectroscopic Signatures of Biofunctionalized SERS Labels

The Raman spectrum of a SERS-labeled antibody together with its schematic structure is shown in Figure 10. The Raman label is a nitro-derivative of mercaptobenzoic acid. Strikingly, only three dominant Raman bands are detected, although the number of atoms in the labeled antibody is very large. No spectral contributions from the antibody, for example the amide I band around 1650 cm^{-1} for α-helices, are observed. This selectivity in the enhancement of Raman bands is primarily due to the SERS distance dependence (cf. Section 2.1): only the Raman label moiety is close enough to the nanoparticle surface to experience the drastic electromagnetic near field enhancement, while the antibody is too distant. A second aspect is the orientation of the Raman label molecules relative to the

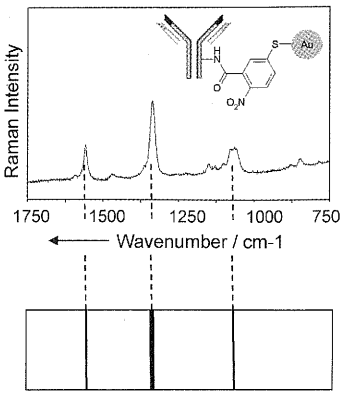

Figure 10. Top: Raman spectrum of a SERS-labeled antibody[6,12] together with its schematic structure (inset). Bottom: In the barcode representation, peak positions and intensities are encoded in the position and the width of the corresponding bar, respectively.

surface normal: according to the SERS selection rules, *z*-components of the molecular polarizability tensor experience the largest enhancement (*z* being the axis parallel to the surface normal). Figure 10 (bottom) shows a barcode representation of the SERS spectrum: peak positions and intensities are encoded in the horizontal position and width of each bar, respectively.

Biofunctionalized SERS probes can be used in applications such as assays or microscopy. The target-specific biomolecule (Table 1) determines the selectivity: for protein recognition, for example, antibodies are often employed. In the following, microscopic applications of SERS for protein localization in cells, tissues and organs are highlighted.

4. Biomedical Applications of SERS Microscopy

4.1. Protein Localization by Immunohistochemistry

The principle of immunohistochemistry for protein localization is schematically illustrated in Figure 11. Usually, either frozen specimens or formalin-fixed and paraffin-embedded tissue samples are used; the latter require techniques for paraffin removal and antigen retrieval. In order to minimize non-specific binding, blocking agents may be employed prior to incuba-

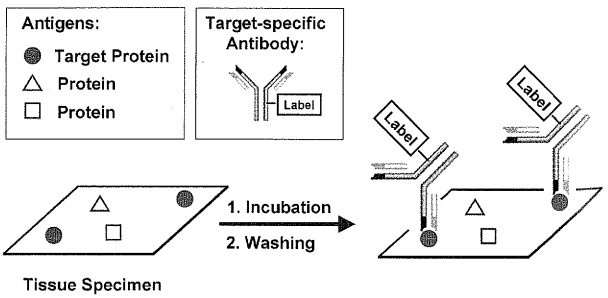

Figure 11. Principle of immunohistochemistry. Left: The antibody selectively recognizes the antigen via its antigen binding sites. Right: After incubation and washing, the antibody-antigen complex is detected by the signal of the label attached to the antibody.

tion. After incubation of the tissue section with labeled antibodies, which leads to the formation of the corresponding antigen-antibody complexes, unbound antibodies are removed by washing. The characteristic signal of the label then allows target protein localization because the label is (often covalently) attached to the antibody, which itself specifically binds to the target protein (Figure 11, right).

Figure 11 shows the use of labeled primary antibodies. An alternative method (not shown) is the subsequent signal amplification by adding labeled secondary antibodies, which specifically bind to the (unlabeled) primary antibody. This approach has been used in combination with SERS, employing CEA (mouse anti-carcinoembryonic antigen) as a primary, and Malachite Green/anti-mouse/gold particles as the secondary antibody, followed by silver staining.[34] Generally, the binding of several secondary antibodies to a single primary antibody leads to a multiplicative signal enhancement. Antigen quantification, however, is generally difficult because of the amplification step. If both quantitative and multiplexed detection in cells and tissue specimens are of interest, the use of SERS-labeled primary antibodies in SERS microscopy is therefore recommended.

4.2. Raman Microspectroscopy and Imaging

Raman microspectroscopy is the combination of optical microscopy with Raman spectroscopy: it enables the spatially resolved detection of Raman spectra from a sample with optical resolution.[35,36] For the acquisition of a complete Raman imaging data set (Figure 12), mapping approaches with point or line focus illumination in combination with a *xy*-translation stage are commonly used. Point mapping allows true confocal Raman microscopy and requires lateral scanning in both the *x* and *y* direction (Figure 12, left). In the line mapping approach, scanning is performed perpendicular to the line focus, that is, only along one spatial dimension (Figure 12, middle). This significantly decreases the number of acquisition steps compared with point mapping, however, confocality in the direction of the line focus is lost.[36] Both, point and line mapping experiments are usually performed with grating-based monochromators. A third, but less often employed methodology is direct imaging: the sample is globally illuminated and filters serve as wavelength selective elements for detecting Raman images at a fixed wavenumber position (Figure 12, right).[36]

Chemical images, which visualize the distribution of a particular chemical component present in the sample, can be generated from the spatially resolved Raman data. In SERS microscopy, which combines Raman microspectroscopy with target-specific SERS probes, the contrast is based on the characteristic signature of the SERS label (cf. Figure 10), usually using either peak intensities or areas encoded in a false-color image. False-color SERS images directly visualize the distribution and concentration of the corresponding target, because SERS signal levels are orders of magnitude more intense than conventional Raman scattering of tissue (cf. Section 2.1),

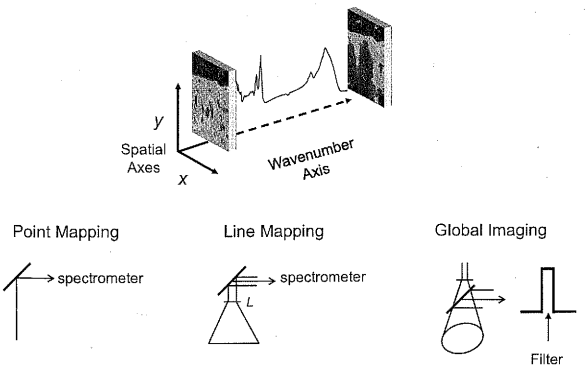

Figure 12. Different methodologies in Raman microspectroscopic imaging.[36] Left: Point mapping. Middle: Line mapping. Both are spectra-based approaches, in which the sample is raster scanned either in two dimensions (point mapping) or one dimension (line mapping). Right: Direct or global imaging projects the sample plane onto the two-dimensional CCD detector and requires wavelength-selective elements such as filters.

4.3. SERS Microscopy: Proof of Principle and First Biomedical Applications

The proof of principle for SERS microscopy using a SERS-labeled primary antibody for target localization in tissue was first demonstrated by Schlücker and co-workers in 2006.[6] Localization of prostate-specific antigen (PSA) in tissue specimens of biopsies from patients undergoing prostatectomy was achieved with SERS-labeled primary PSA antibodies, gold/silver nanoshells, aromatic Raman labels and red laser excitation (632.8 nm). PSA was chosen as a target protein because of its high expression level in prostate tissue and its selective histological abundance in the epithelium of the prostate gland. The combination of gold/silver nanoshells as a SERS substrate and red laser excitation reduces autofluorescence of tissue specimens and thereby increases the signal and image contrast. In the incubated prostate tissue section, SERS from aromatic Raman labels attached to gold/silver nanoshells was detected only in the PSA-(+) epithelium (Figure 13, A–C); the PSA-(−)

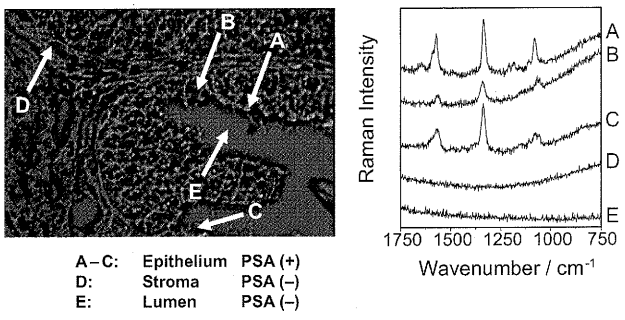

Figure 13. Proof of principle for SERS microscopy using SERS-labeled primary antibodies for tissue diagnostics.[6] Prostate-specific antigen (PSA) as the target protein was localized in biopsies from patients with prostate cancer. Left: Prostate tissue contains different histological classes such as epithelium, stroma and lumen, in which PSA is either abundant (+) or not (−). Top right: SERS-labeled anti-PSA antibodies are detected in the PSA-(+) epithelium, showing the characteristic Raman signals of the SERS label. Bottom right: Locations in the PSA-(−) stroma and lumen serve as negative controls where no spectral contributions of the SERS-labeled antibody are detected.

stroma and lumen served as negative controls (Figure 13, D–E).[6] The SERS signal of a complete SAM of Raman reporters on gold/silver nanoshells upon red laser excitation is ~180 times higher than for submonolayer coverage on solid gold nanospheres of the same size.[18]

Further applications of SERS microscopy for cellular and tissue diagnostics appeared soon after. For the localization of two targets (HER2 and CD10) on cellular membranes, glass-coated assemblies (see Section 3.2.2) were used as SERS probes.[15] Employing SERS imaging with Au/Ag core–shell nanoparticles, the overexpression of phospholipase Cγ1 in human embryonic kidney (HEK 293) cells was demonstrated.[37] In a study of mammalian cell surface receptors, the role of small aggregated nanoparticle clusters was elucidated with SERS microscopy in combination with scanning electron microscopy (SEM). The strongest SERS signals originate from aggregates oriented in the appropriate direction with respect to the polarization of the incident laser.[38] Also COINs (see Section 3.2.2) were used as SERS probes for PSA localization in sections of prostate tissue.[39] The issue of steric hindrance was analyzed in a simultaneous two-COIN staining for PSA: each of the two distinct Raman labels was conjugated separately to a PSA antibody, yielding two distinct biofunctionalized SERS labels with PSA antibodies on their surface. The characteristic Raman signatures from both COINs were detected at almost every location in the epithelium, suggesting that steric hindrance from COINs does not represent a major problem. In a subsequent study, the same group presented a detailed comparison of the staining performance with SERS- and fluorophore-PSA antibody conjugates on adjacent tissue sections.[40] Staining with COIN- and Alexa-fluorophore labeled antibodies yielded similar results, with a lower staining accuracy but comparable signal intensities for COINs. The spectral analysis in both experiments demonstrated the fundamental difference in a Raman/SERS-based versus a molecular fluorophore-based detection: the narrow Raman signals of the SERS probes can clearly be discriminated from background autofluorescence, which is particularly advantageous for low-abundant analytes and low-intensity signals. Depending on the quality of the spectra and the degree of spectral overlap between the SERS label signatures, appropriate mathematical algorithms for signal decomposition must be employed.[41]

4.4. Multiplexing and Quantification with SERS Labels

Generally, the term multiplexing refers to the parallel determination of several parameters within a single experiment. In the context of SERS as a labeling strategy for targeted research, multiplexing addresses the issue of simultaneously detecting and identifying the spectral fingerprint of several distinct SERS labels. As an example, Figure 14 shows the Raman spectra of five different SERS labels, each of them containing a complete SAM of arylthiols on gold nanospheres.

Table 2 shows the multiplexing capacity of dyes, fluorophores and SERS labels. The characteristic electronic absorption of a dye in the UV/Vis spectral region is often used as a readout signal. Due to the broad electronic absorption bands

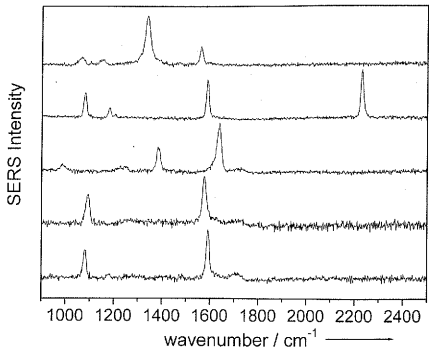

Figure 14. Raman spectra of five distinct SERS labels for multiplexing, each of them comprising a complete SAM of arylthiols on gold nanospheres.

Table 2. Multiplexing capacity of different labeling approaches. In addition to the type of label, the underlying physical processes are specified. SERS labels offer unique multiplexing capacities compared with existing techniques based on electronic absorption or emission spectroscopies.

Process	Label	Multiplexing Capacity
Electronic absorption	Dyes	~1–3
Flurorescence emission	Molecular fluorophores	~1–3
	Quantum dots	~3–10
Raman scattering	SERS labels	~10–100

and their spectral overlap, the multiplexing capacity is limited to approx. 1–3. The same argument also applies to fluorescence emission signals of molecular fluorophores. The introduction of quantum dots, that is, nanocrystalline semiconductors with bright fluorescence signals, has been a major improvement in the multiplexing capacity of fluorescence-based detection schemes: approx. 3–10 quantum dots may be detected simultaneously because of the narrower emission peaks compared with molecular fluorophores.[42] The linewidth of vibrational Raman bands is even significantly smaller: typically two orders of magnitude or more compared with molecular fluorophores. Considering that only selected Raman bands are observed in the SERS spectra of SERS labels (cf. Figure 10 top), the multiplexing capacity of SERS can be estimated: 10–30 different SERS labels seems realistic for microscopic applications, while 100 is considered to be a theoretical upper limit.

Multiplexing was first demonstrated in SERS applications for the detection of DNA and proteins in solution. Mirkin and co-workers performed multiplexed (6-plex) detection of DNA, employing a three-component sandwich assay in a microarray format.[11] Commercially available dyes were used as Raman labels: Cy3, Cy3.5, Cy5, rhodamine 6G, tetramethyl rhodamine and texas red. Graham and co-workers have also performed multiplexed experiments for DNA detection, using either custom-made benzotriazoles[43] or further commercially available dyes, including BODIPY, Cy5.5, FAM and ROX.[44–46] In contrast to studies in solution, only very few multiplexed SERS microscopic experiments in tissues have been performed.[41,47]

In addition to the multiplexing capacity, quantification is a further very important aspect in bioanalytical applications. Vari-

ous groups have demonstrated that the SERS signal response is proportional to the amount of SERS label.[29,47] In a series of studies the ability of SERS or SERRS for quantifying the concentration of DNA[46] and proteins[39] was demonstrated.

4.5. In vivo SERS

In 2008 the first application of SERS for in vivo tumor targeting has been demonstrated by Nie and co-workers.[48] Colloidal gold covered with Crystal Violet and thiol-modified polyethylene glycols (PEGs) was used as a SERS label. The authors estimate that about $1.4–1.5\times10^4$ Raman reporter molecules and about 3.0×10^4 thiol-PEG molecules are present on the surface of a 60 nm gold particle, that is, the surface coverage with Raman labels is ca. 30% (see Section 3.2.1). The heterofunctional PEG spacer allows further bioconjugation. For tumor recognition, the SERS label was conjugated to a single-chain variable fragment antibody. This fragment binds selectively to the epidermal growth factor receptor which is overexpressed in many human malign tumors. SERS-labeled antibodies were detected in vivo after injection into the tail vein of a mouse model. Tumor-specific recognition was demonstrated by control experiments in which the SERS labels were not conjugated to the antibody fragment. In comparison with quantum dots emitting in the NIR, the SERS labels yielded a ca. 200 times more intense signal.

Soon after, Gambhir and co-workers demonstrated multiplexed in vivo SERS microscopy in mice using pegylated and non-pegylated silica-coated gold particles with sub-monolayer coverage of Raman reporter molecules (see Section 3.2.1) as SERS probes, that is, without a target-specific (bio)molecule.[47] After tail vein injection, liver pharmacokinetics was investigated and it was found that both PEG and nonpegylated probes show no difference in liver accumulation. The authors note that in vivo SERS microscopy may complement other imaging (also non-optical) strategies such as radiology. Potential limitations have to be investigated in future studies with SERS probes, including problems with delivery due to nanoparticle size, the optimal injected dose and the potential toxicity of the particles.[47–48] Due to the photothermal effect,[49,50] the particles could also be used for therapeutic purposes in addition to diagnostics.[48]

5. Summary and Outlook

SERS microscopy is a novel and very promising approach for targeted research, in particular because of its immense multiplexing capacity for simultaneous target localization in combination with quantification (see Figure 15). Numerous applications for the analysis of cells and tissues are expected to appear within the next years. Cancer diagnostics will certainly be an important field where this innovative methodology offers significant advantages over existing approaches.

Further studies are needed to evaluate the advantages and disadvantages of SERS microscopy compared to other optical techniques, in particular fluorescence microscopy employing molecular fluorophores and quantum dots. For all in vivo experiments with nanoparticles including SERS labels, biodistribution and toxicity have to be investigated.[47–48]

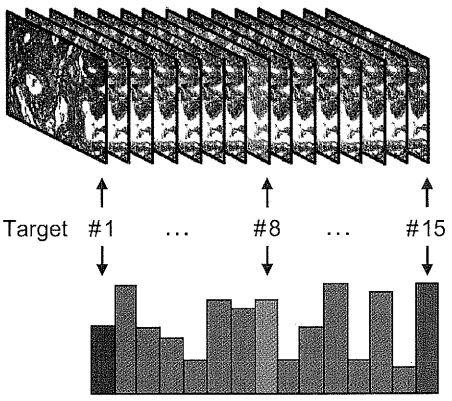

Figure 15. SERS microscopy has the potential for the detection of multiple targets (multiplexing) and their quantification, two important aspects for tissue diagnostics.

Advantages of SERS labels are first the high multiplexing capacity, second the ability to quantify the target concentration combined with high sensitivity, and third their photostability. High quality data, in particular the ability to clearly distinguish the SERS signals from background autofluorescence are also an important aspect. A disadvantage may be the relatively large size of SERS labels compared with molecular fluorophores. For surface antigens, cell and tissue sections as well as assays, however, this is not critical. The simultaneous detection (assays) or localization (microscopy) of multiple target molecules is time- and cost-saving. Additionally, smaller sample volumes are required. The largest impact may therefore be expected for in vitro diagnostic (IVD) applications.

Several groups worldwide are actively working on improved designs of SERS probes with high sensitivity and reproducible signals. Also, the number of biomedical SERS applications is constantly increasing. Commercially available SERS labels together with standardized conjugation protocols will probably play an important role in the future because they help the practitioner to focus on applications rather than on the chemical synthesis and characterization of SERS probes.

Advances in laser, filter, spectrometer and detector technology contributed to the fact that Raman including SERS spectroscopy is now a mature analytical technique. Easy to use commercial equipment permits to perform experiments without an in-depth knowledge of optics and lasers. For Raman microscopy, extremely fast Raman systems equipped with motorized *xy*-stages are now commercially available, enabling data acquisition down to only few milliseconds or even sub-milliseconds per pixel.

Eighty years after the discovery of the Raman effect, conventional Raman scattering has already made the transition to the clinics, for example, in the area of bacteria identification or in surgery for online monitoring by fiber optic probes. The next years will show whether SERS in targeted research as a relatively new approach will experience a similar success story. I'm optimistic that SERS will establish itself in certain areas; one

should keep in mind, however, that it usually takes several years until a new technology becomes widely accepted. Joint efforts between Raman spectroscopists, synthesis chemists, biologists and medical doctors as well as close international collaborations will be necessary to achieve this goal.

Acknowledgements

Financial support from the German Research Foundation (DFG; SCHL 594/4-1, Heisenberg fellowship SCHL 594/5-1, SFB 630/C1) and the German Ministry of Education and Science (BMBF; EXIST Seed) is highly acknowledged. I am indebted to my graduate students Magdalena Gellner, Bernd Küstner, Stephan Niebling, Mohammad Salehi and Max Schütz for carefully reading the manuscript, for their critical comments and to M. G. also for preparing several figures. The laboratory work of many students during their summer internships and diploma theses is also acknowledged.

Keywords: lasers · metals · microscopy · proteins · Raman spectroscopy

[1] R. Aroca, *Surface-Enhanced Vibrational Spectroscopy*, Wiley, New York, **2006**.
[2] *Surface-Enhanced Raman Scattering: Physics and Applications* (Eds.: K. Kneipp, M. Moskovits, H. Kneipp), *Topics in Applied Physics*, Vol. 103, Springer, Berlin, **2006**.
[3] P. L. Stiles, J. A. Dieringer, N. C. Shah, R. P. Van Duyne, *Annu. Rev. Anal. Chem.* **2008**, *1*, 601–626.
[4] "Selective Detection of Proteins and Nucleic Acids with Biofunctionalized SERS Labels": S. Schlücker, W. Kiefer in *Frontiers of Molecular Spectroscopy* (Ed.: J. Laane), Elsevier, Amsterdam, **2009**, pp. 267–288.
[5] M. D. Porter, R. J. Lipert, L. M. Siperko, G. Wang, R. Narayanan, *Chem. Soc. Rev.* **2008**, *37*, 1001–1011.
[6] S. Schlücker, B. Küstner, A. Punge, R. Bonfig, A. Marx, P. Ströbel, *J. Raman Spectrosc.* **2006**, *37*, 719–721.
[7] W. E. Doering, M. E. Piotti, M. J. Natan, R. G. Freeman, *Adv. Mater.* **2007**, *19*, 3100–3108.
[8] *Immunoassay and Other Bioanalytical Techniques* (Ed.: J. M. Van Emon), CRC Press, Boca Raton, **2007**.
[9] J. Ni, R. J. Lipert, G. B. Dawson, M. D. Porter, *Anal. Chem.* **1999**, *71*, 4903–4908.
[10] D. Graham, B. J. Mallinder, W. E. Smith, *Biopolymers* **2000**, *57*, 85–91.
[11] Y. C. Cao, R. Jin, C. A. Mirkin, *Science* **2002**, *297*, 1536–1540.
[12] D. S. Grubisha, R. J. Lipert, H.-Y. Park, J. Driskell, M. D. Porter, *Anal. Chem.* **2003**, *75*, 5936–5943.
[13] Y. C. Cao, R. Jin, J.-M. Nam, C. S. Thaxton, C. A. Mirkin, *J. Am. Chem. Soc.* **2003**, *125*, 14676–14677.
[14] X. Su, J. Zhang, L. Sun, T.-W. Koo, S. Chan, N. Sundararajan, M. Yamakawa, A. A. Berlin, *Nano Lett.* **2005**, *5*, 49–54.
[15] J.-H. Kim, J.-S. Kim, H. Choi, S.-M. Lee, B.-H. Jun, K.-N. Yu, E. Kuk, Y.-K. Kim, D. H. Jeong, M.-H. Cho, Y.-S. Lee, *Anal. Chem.* **2006**, *78*, 6967–6973.
[16] R. Jin, Y. C. Cao, C. S. Thaxton, C. A. Mirkin, *Small* **2006**, *2*, 375–380.
[17] M. Yang, T. Chen, W. S. Lau, Y. Wang, Q. Tang, Y. Yang, H. Chen, *Small* **2009**, *5*, 198–202.
[18] B. Küstner, M. Gellner, M. Schütz, F. Schöppler, A. Marx, P. Ströbel, P. Adam, C. Schmuck, S. Schlücker, *Angew. Chem.* **2009**, *121*, 1984–1987; *Angew. Chem. Int. Ed.* **2009**, *48*, 1950–1953.
[19] C. J. Murphy, T. K. Sau, A. M. Gole, C. J. Orendorff, J. Gao, L. Gou, S. E. Hunyadi, T. Li, *J. Phys. Chem. B* **2005**, *109*, 13857–13870.
[20] Y. Xia, Y. Xiong, B. Lim, S. E. Skrabalak, *Angew. Chem.* **2009**, *121*, 62–108; *Angew. Chem. Int. Ed.* **2009**, *48*, 60–103.
[21] Y. Sun, B. T. Mayers, Y. Xia, *Nano Lett.* **2002**, *2*, 481–485.
[22] M. Gellner, B. Küstner, S. Schlücker, *Vib. Spectrosc.* **2009**, *50*, 43–47.
[23] G. Mie, *Ann. Phys.* **1908**, *330*, 377–445.
[24] C. F. Bohren, D. R. Huffman, *Absorption and Scattering of Light by Small Particles*, Wiley-VCH, Weinheim, **1998**.
[25] S. J. Oldenburg, S. L. Westcott, R. D. Averitt, N. J. Halas, *J. Chem. Phys.* **1999**, *111*, 4729–4735.
[26] Y. Cui, B. Ren, J.-L. Yao, R.-A. Gu, Z.-Q. Tian, *J. Phys. Chem. B* **2006**, *110*, 4002–4006.
[27] N. R. Jana, *Analyst* **2003**, *128*, 954–956.
[28] A. F. McCabe, C. Eliasson, R. A. Prasath, A. Hernandez-Santana, L. Stevenson, I. Apple, P. A. G. Cormack, D. Graham, W. E. Smith, P. Corish, S. J. Lipscomb, E. R. Holland, P. D. Prince, *Faraday Discuss.* **2006**, *132*, 303–308.
[29] S. P. Mulvaney, M. D. Musick, C. D. Keating, M. J. Natan, *Langmuir* **2003**, *19*, 4784–4790.
[30] W. Stöber, A. Fink, E. Bohn, *J. Colloid Interface Sci.* **1968**, *26*, 62–69.
[31] W. E. Doering, S. Nie, *Anal. Chem.* **2003**, *75*, 6171–6176.
[32] K. Kneipp, Y. Wang, R. R. Dasari, M. S. Feld, *Appl. Spectrosc.* **1995**, *49*, 780–784.
[33] G. T. Hermanson, *Bioconjugate Techniques*, Academic Press, San Diego, **2008**.
[34] D. A. Stuart, A. Haes, A. D. McFarland, S. Nie, R. P. Van Dyne, *Proc. SPIE-Int. Soc. Opt. Eng.* **2004**, *5327*, 60–73.
[35] *Raman Microscopy: Developments and Applications* (Eds.: G. Turrell, J. Corset), Academic Press, San Diego, **1996**.
[36] S. Schlücker, M. D. Schaeberle, S. W. Huffmann, I. W. Levin, *Anal. Chem.* **2003**, *75*, 4312–4318.
[37] S. Lee, S. Kim, J. Choo, S. Y. Shin, Y. H. Lee, H. Y. Choi, S. Ha, K. Kang, C. H. Oh, *Anal. Chem.* **2007**, *79*, 916–922.
[38] Q. Hu, L.-L. Tay, M. Noestheden, J. P. Pezacki, *J. Am. Chem. Soc.* **2007**, *129*, 14–15.
[39] L. Sun, K.-B. Sung, C. Dentinger, B. Lutz, L. Nguyen, J. Zhang, H. Qin, M. Yamakawa, M. Cao, Y. Lu, A. J. Chmura, J. Zhu, X. Su, A. A. Berlin, S. Chan, B. Knudsen, *Nano Lett.* **2007**, *7*, 351–356.
[40] B. Lutz, C. Dentinger, L. Sun, L. Nguyen, J. Zhang, A. J. Chmura, A. Allen, S. Chan, B. Knudsen, *J. Histochem. Cytochem.* **2008**, *56*, 371–379.
[41] B. R. Lutz, C. E. Dentinger, L. N. Nguyen, L. Sun, J. Zhang, A. N. Allen, S. Chan, B. S. Knudsen, *ACS Nano* **2008**, *2*, 2306–2314.
[42] X. Michalet, F. F. Pinaud, L. A. Bentolila, J. M. Tsay, S. Doose, J. J. Li, G. Sundaresan, A. M. Wu, S. S. Gambhir, S. Weiss, *Science* **2005**, *307*, 538–544.
[43] D. Graham, K. Faulds, W. E. Smith, *Chem. Commun.* **2006**, 4363–4371.
[44] D. Graham, W. E. Smith, A. M. T. Linacre, C. H. Munro, N. D. Watson, P. C. White, *Anal. Chem.* **1997**, *69*, 4703–4707.
[45] D. Graham, B. J. Mallinder, W. E. Smith, *Angew. Chem.* **2000**, *112*, 1103–1105; *Angew. Chem. Int. Ed.* **2000**, *39*, 1061–1063.
[46] K. Faulds, F. McKenzie, W. E Smith, D. Graham, *Angew. Chem.* **2007**, *119*, 1861–1863; *Angew. Chem. Int. Ed.* **2007**, *46*, 1829–1831.
[47] S. Keren, C. Zavaleta, Z. Cheng, A. de la Zerda, O. Gheysens, S. S. Gambhir, *Proc. Natl. Acad. Sci. USA* **2008**, *105*, 5844–5849.
[48] X. Qian, X.-H. Peng, D. O. Ansari, Q. Yin-Goen, G. Z. Chen, D. M. Shin, L. Yang, A. N. Young, M. D. Wang, S. Nie, *Nat. Biotechnol.* **2008**, *26*, 83–90.
[49] L. R. Hirsch, R. J. Stafford, J. A. Bankson, S. R. Sershen, B. Rivera, R. E. Price, J. D. Hazle, N. J. Halas, J. L. West, *Proc. Natl. Acad. Sci. USA* **2003**, *100*, 13549–13554.
[50] X. Huang, I. H. El-Sayed, W. Qian, M. A. El-Sayed, *J. Am. Chem. Soc.* **2006**, *128*, 2115–2120.

Received: February 16, 2009

